FULL PAPER

Density Functional Study of the Reaction Mechanism of Two Oxiimine Alcohol Formations and Their Novel Rearrangements

by **Yunus Kaya**

Department of Chemistry, Faculty of Arts and Sciences, Uludag University, TR-16059 Bursa, Turkey
(phone: +90-224-2941738; e-mail: ykaya@uludag.edu.tr)

In this study, the reaction mechanisms of isonitrosoacetophenone (inapH) with ethanolamine (ea) and 1-phenylethanolamine (pea) have been investigated theoretically using B3LYP/6-311G(d,p) method to explain why the formation and unexpected rearrangement products occur or not occur. While the reaction between isonitrosoacetophenone (inapH) with ethanolamine gives oximine alcohol (**Ib**), the reaction of 1-phenylethanolamine with inapH results in the formation of oximine alcohol with a different substituent (**Ia**) and amido alcohol (**IIa**), which is the unexpected rearrangement product. The rearrangement driving forces of compounds from **Ia** to **IIa** are calculated as *ca*. 28 and 23 kJ/mol in the gas and EtOH phases, respectively. These driving forces have been calculated *ca*. 46 and 45 kJ/mol for the rearrangement of compound **Ib** to obtain **IIb** in the same phases, respectively. This high driving force shows that the compound **IIb** cannot be obtained from rearrangement of compound **Ib** as described experimentally in the literature. In addition, as the DFT functionals poorly describe dispersion effects, dispersion correction for reaction heat and free-energy barrier was estimated using the wB97X-D/6-311G(d,p). In general, the relative free energies of all molecules calculated from wB97XD method are lower than performed from B3LYP level. The changes of thermodynamic properties for all molecules with temperature ranging from 100 to 500 K have been obtained using the statistical thermodynamic method.

Keywords: Mechanism, Oxiimine alcohol, Amido alcohol, DFT Calculations, NBO Analysis.

Introduction

The imine oximes contain both oxime and imine nitrogen atoms and commonly used as bidentate ligands [1]. The reactivity of the oxime group and its metal coordination capability have been studied experimentally and well documented in the literature [1 – 14]. Isomerization [15 – 28] reaction mechanisms [29 – 32] and spectroscopic studies of some oximes were also performed theoretically [33 – 41]. *Schiff* bases are well-known compounds and are commonly used in industrial and biological area as a reaction intermediate. The possible reaction mechanism of the *Schiff* base formation and the effect of the solvent effect, pH, and type of reactants have also been explained theoretically [42 – 49].

On the other hand, amides are important building blocks in organic and material chemistry as they are widely employed not only in plastic, rubber, paper, and color industry (crayons, pencils, and inks), but also in water and sewage treatment [50 – 52]. Furthermore, numerous pharmaceutical molecules incorporate amides as core unit; *N*-acetyl-4-aminophenol and local anesthetic lidocaine and dibucaine are just a few examples [50 – 53]. Thus, considering their importance as intermediate in the industry and as precursors in drug formulation, the development of simpler and more economical process for amide synthesis has been of great interest over the last 20 years [54].

Among the most commonly used synthetic approaches for these compounds, many involve the reaction of amine with anhydrides, acyl chlorides, or, in some cases, with the acid itself [50]. This latter approach results in the complete conversion of the substrate only when the water formed during the reaction is continuously removed [50]. Amides can also be synthesized by a two-step reaction: oximation of ketones, a quite facile reaction generally carried out with hydroxylamine hydrochloride or sulfate in an aqueous or H_2O–EtOH solution, followed by *Beckmann* rearrangement in mineral acids [53 – 59]. The first step proceeds in the presence of a base to allow the formation of the free hydroxylamine that, then, attacks the C=O group of the ketone. On the other hand, *Beckmann* rearrangement is generally carried out in mineral acid, *i.e.*, H_2SO_4 or oleum [54 – 60], for which safety and/or disposal problems must be taken into account especially in the industrial practice [61 – 66]. Furthermore, the resulting amides are protonated, thus, dilution with H_2O or neutralization of the acid (typically with aqueous ammonia) is required to recover the pure product [61 – 66]. This procedure is used in the industrial synthesis of caprolactam, which is the

DOI: 10.1002/hlca.201500155

monomer of nylon [61 – 66]. Nowadays, the oximation-rearrangement sequence in oleum is superseded by the *Enichem–Sumitomo* processes consisting of liquid-phase ammoximation [62] followed by a gas-phase *Beckmann* rearrangement [63 – 66]. Another interesting approach to amide synthesis is to use ionic liquids in combination with *Lewis* acids. This procedure results in a high-yielding *Beckmann* rearrangement for some activated oximes [67][68]. The process, however, requires a preliminary oximation stage and a tedious workup for both oximation and *Beckmann* rearrangement. However, the rearrangement reactions of imine oximes have not been found in the literature.

Recently, we synthesized oxiimine alcohols, namely (3*E*)-3-aza-5-(hydroxyimino)-1,4-diphenylpent-3-en-1-ol (**Ia**) [69] and (1*E*,2*E*)-[(2-hydroxyethyl)imino]-2-phenylethanal oxime (**Ib**) [70]. During the preparation of the compound **Ia**, we observed that the amido alcohol (**IIa**) was obtained as associated product interestingly. The amido alcohol (**IIa**) was characterized by single-crystal X-ray diffraction [69]. But the compound **IIb** could not be obtained in the synthesis of compound **Ib** [70]. The aim of this work is to study the formation mechanism of oxiimine alcohols, namely **Ia** and **Ib**. In addition, the formation mechanisms of amido alcohols (**IIa** and **IIb**) (rearrangements of oxiimine alcohols) were investigated theoretically and the substituent effect of the rearrangement of oxiimine alcohol was studied. For this purpose, density functional theory (DFT) calculations at the *Becke–Lee–Yang–Parr* (B3LYP)/6-311G(d,p) level of theory and integral equation formalism variant of the polarizable continuum model (IEFPCM) were performed to explain the formation mechanisms of the oxiimine alcohols (**Ia** and **Ib**) and amido alcohols (**IIa** and **IIb**). This theoretical study is the first example of such interesting rearrangement of imine oximes. Therefore, this study will lead researchers working theoretical imine oxime or oxime mechanism.

Results and Discussion

In our previous study, a new reaction has been found between isonitrosoacetophenone (inapH) and 1-phenylethanol amine (pea) [69]. The oxiimine alcohol (**Ia**), namely (3*E*)-3-aza-5-(hydroxyimino)-1,4-diphenylpent-3-en-1-ol monohydrate was synthesized by the reaction of inapH with pea in a moderate yield (50%). After separating the oxiimine alcohol (**Ia**) from the reaction mixture, the filtrate was evaporated, and then the oily product was recrystallized, so the unexpected product, amido alcohol (**IIa**), was obtained at very low yield (9%). In addition, as a result of the reaction of inapH with ethanol amine (ea) only oxiimine alcohol (**Ib**), namely (1*E*,2*E*)-[(2-hydroxyethyl)imino]-2-phenylethanal oxime was synthesized (yield, 87%) and amido alcohol (**IIb**) could not be obtained [70]. Compound **IIa** was obtained as a single crystal, while compound **Ia** and **Ib** were synthesized as a polycrystalline powder. Thus, the structures of **Ia** and **Ib** were supported by spectroscopic methods and LC/MS technique [69][70]. In this study, the reaction mechanisms of inapH with pea and ea, and rearrangement of compounds **Ia** and **Ib** were studied theoretically. The reactions of inapH with pea and ea subjected to the theoretical analysis are given in the *Scheme*. The formation of compound **I** occurs in two steps, while that of compound **II** takes place in three steps. The structures of **I** and **II** are very flexible and represent several conformations. To establish the most stable conformation, the molecule was subjected to a rigorous conformation analysis around the free rotation bonds. The structure of **Ia** represents several conformations as illustrated in *Fig. S1*. The (*E*)- and (*Z*)-isomers of the **Ia** display *s-cis* and *s-trans* conformations. The energies of the studied isomers are listed in *Table 1*. In the gas phase, the *s-trans*-(*E*,*E*)-isomer is the most stable one, while the *s-cis*-(*Z*,*E*)-

Scheme. Synthesis reaction of compounds **I** and **II**

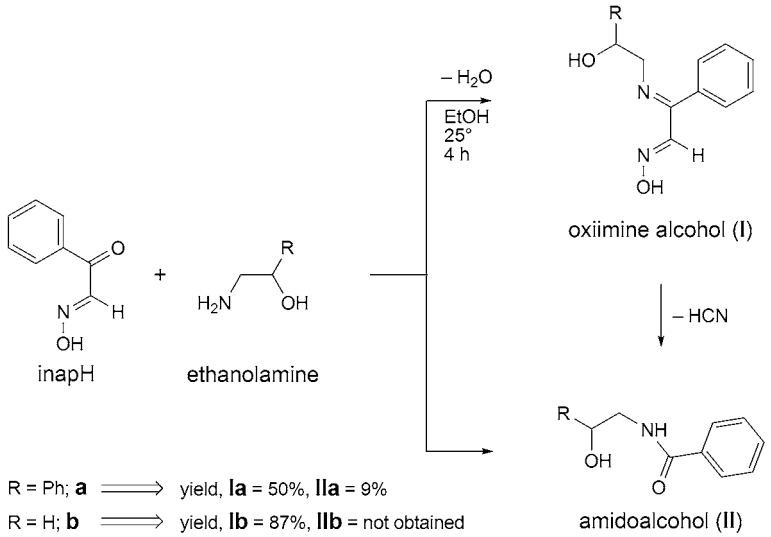

Table 1. Calculated relative energies, dihedral angles, and dipole moments of the isomers of compound **Ia**

Isomers			Dihedral angles N1–C1–C2–N2	ΔE [kJ/mol]
s-trans	(*E*)	(*E*)	177.3	0.00
s-trans	(*E*)	(*Z*)	−177.8	5.80
s-trans	(*Z*)	(*E*)	158.9	18.23
s-trans	(*Z*)	(*Z*)	−127.8	15.00
s-cis	(*E*)	(*E*)	32.6	19.95
s-cis	(*E*)	(*Z*)	4.5	7.19
s-cis	(*Z*)	(*E*)	68.1	28.22
s-cis	(*Z*)	(*Z*)	−63.1	21.31

isomer is the less stable. Therefore, the optimized molecular structure of the most stable isomer (*s-trans*-(*E*,*E*)) is used for all calculations. Similar calculations were also made for **Ib** in our previous study [70]. Tautomers are structural isomers that are conceptually related by the shift of hydrogen and one or more bonds. Amide–iminol tautomerization is an analogue of the well-known *keto–enol* tautomerization. *Keto–enol* tautomerism in **IIa** was studied using B3LYP/6-311G(d,p) method. Relative free energies of isodesmic reaction for *keto–enol* are calculated at 71.72 kJ/mol (*Fig. S2*). This result showed that the *keto* tautomer is more stable than *enol* tautomer in the gas phase for **IIa**. The optimized geometry of **IIa** obtained by

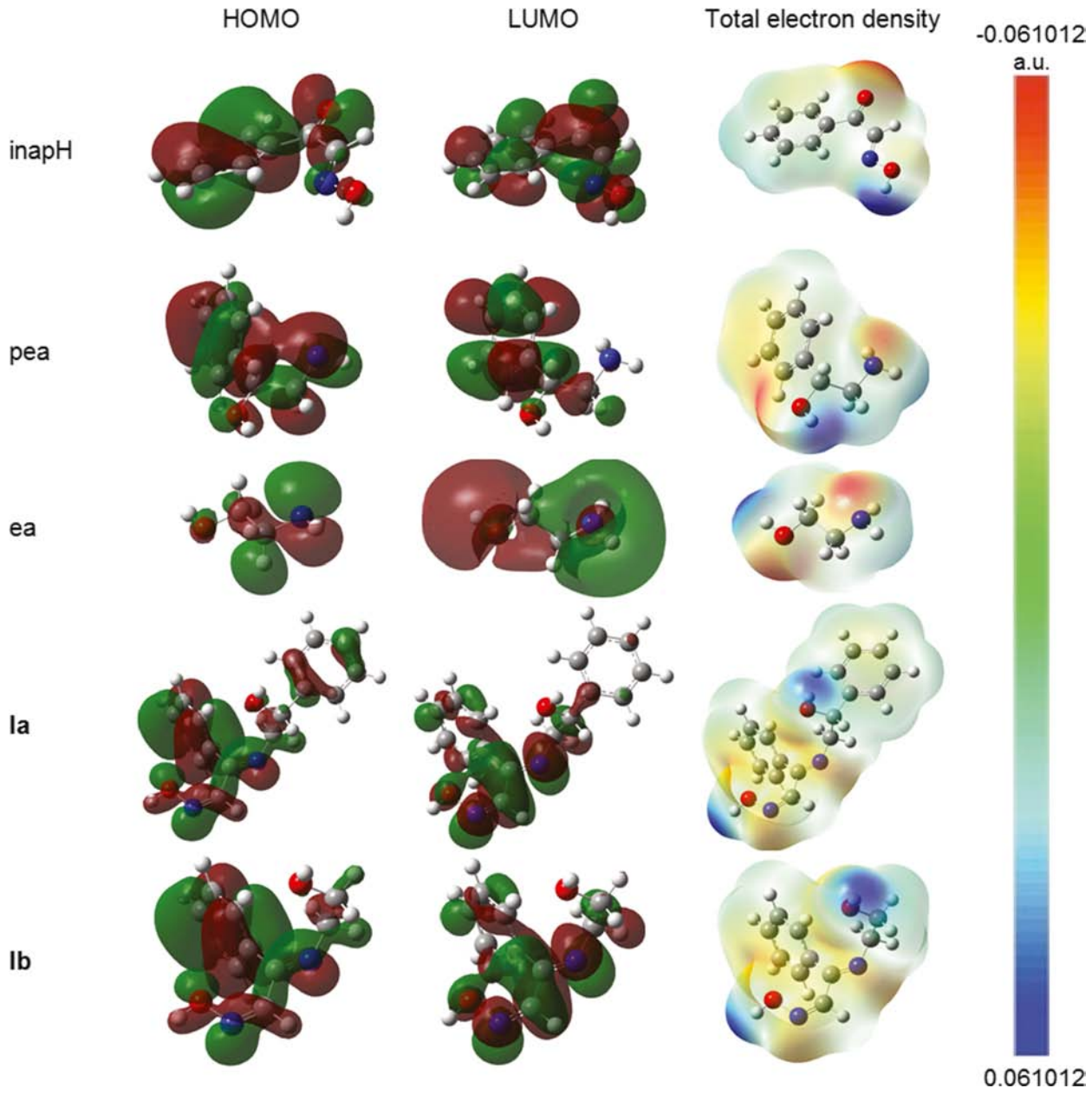

Fig. 1. HOMO, LUMO molecular orbitals, and total electron density for inapH, pea, ea, **Ia**, and **Ib** (The electron-rich region is coded red color, while the electron-poor region is blue color on the total electron density surface).

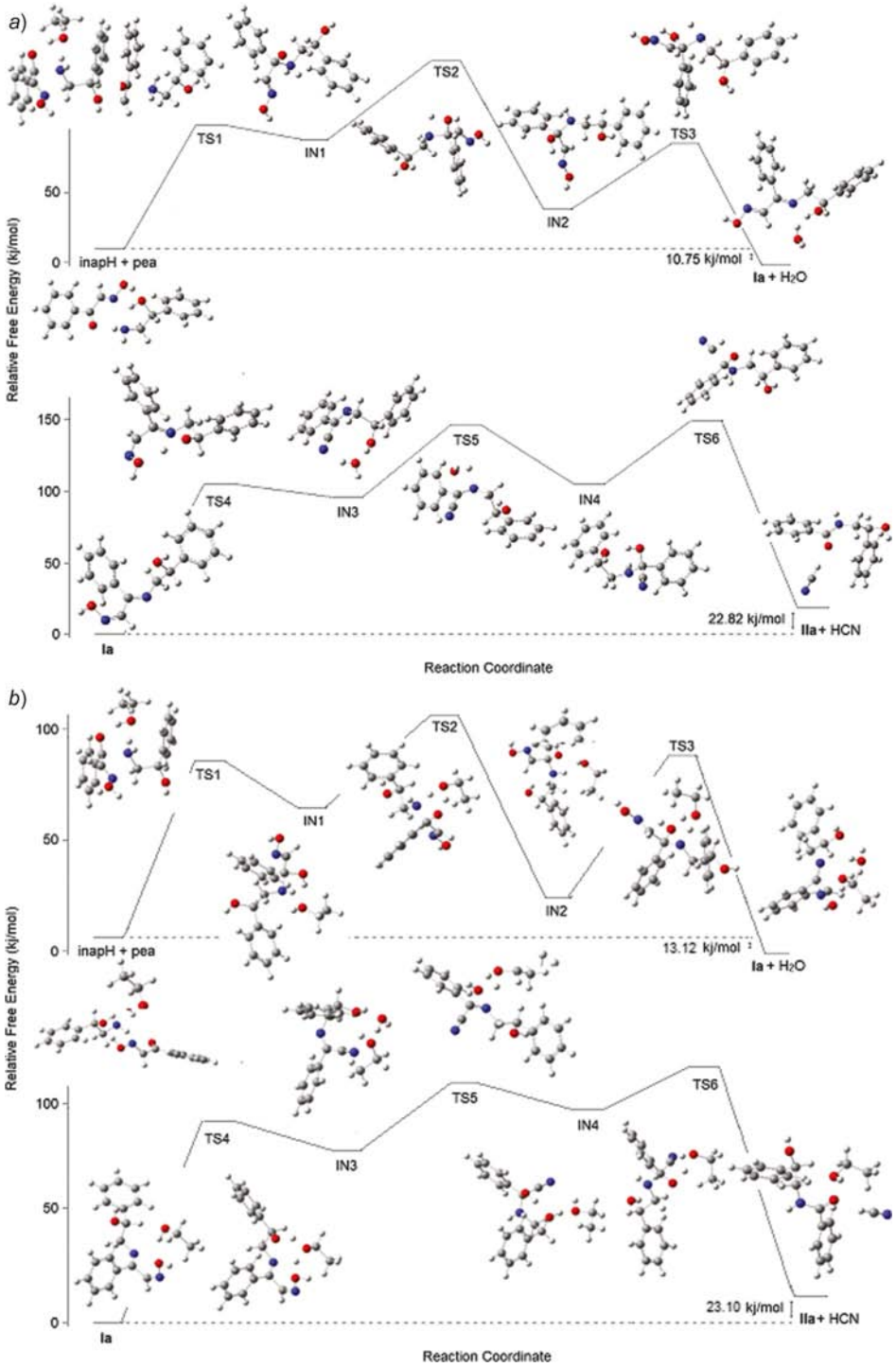

Fig. 2. The potential energy diagram and geometry transformations, showing the formation of compound **Ia**, **IIa**, and optimized geometries of the reactants, intermediates, transition states, and products calculated by B3LYP/6-311G(d,p), *a*) without solvent molecule, *b*) added solvent molecule.

B3LYP/6-311G(d,p) method was used for conformational analysis, which was performed by potential energy surface scan function using same basis set. The different conformers of the compound were obtained by varying the dihedral angle O(2)–C(2)–N(2)–C(9) in the steps of 36° over one complete rotation from 0° to 360°. The graphical output, drawn between total energy *vs.* scan coordinates, of this conformer analysis is presented in *Fig. S3*. The graph clearly shows that there is a conformer with minimum energy at 357°. The structure of the molecule at this conformation is shown in *Fig. S3* representing the minimum energy conformer or the most stable conformer of this compound.

The HOMO, LUMO orbital visualizations, and total electron density surfaces of inapH, pea, ea, **Ia**, and **IIa** are given in *Fig. 1*, while the compositions of the HOMO and LUMO orbitals are listed in *Table S1*. As seen from the figure and table, while the HOMO orbital of the inapH molecule is mostly localized on C=O (22%) and phenyl (67%) groups, amine groups have the highest contributions at the pea (38%) and ea (79%) molecules. The LUMO orbital contributions of inapH, pea, and ea molecules are generally separated from all parts of the molecules, except amine group of pea. For the HOMO orbitals of **Ia** – **Ib**, the contributions of the imine oxime, and phenyl groups were 23 – 21% and 45 – 65%, respectively. On the other hand, LUMO orbitals of **Ia** and **Ib** were dominantly localized on imine oxime groups, *ca.* 82% and 68%, respectively. The electron-rich and electron-poor regions are given with red and blue colors on the total electron density surface, respectively. Most electron contributions were observed on the C=O oxygen of the inapH. In the pea and ea molecules, the electron-poor regions are the hydrogen atoms of the NH_2 groups, meaning that electrons were accumulated mostly on the nitrogen atom. In addition, the electron-rich regions are the oxygen atoms of oxime groups, while the electron-poor regions are the hydrogen atoms of the OH groups in **Ia** and **IIa**.

Formation of Compound **Ia**

All calculations of mechanisms were performed in two ways: the first one is only in the presence of reactants, which are C=O oxime and amine, and the second one is also the participation of solvent molecule in the mechanism. The mechanism of the formation reaction of compound **Ia** involves two steps, namely: *i*) formation of a carbinolamine intermediate (inapH + pea-IN2 in *Fig. S4*), and *ii*) dehydration of the carbinolamine to give the final imine (oxiimine alcohol, **Ia**) (TS3-**IIa** + H_2O in *Fig. S4*). The corresponding potential energy surfaces (PES's) and optimized structures of all molecules for formation reaction of the compounds **Ia** and **IIa** are shown in *Fig. 2*, while relative enthalpies and free energies of the reactants, intermediates (IN), transition states (TS), and products are given in *Table 2*

Table 2. Relative enthalpy, relative free energy, and negative frequency of the structures of the reaction paths for gas phase and EtOH solution of compound **Ia** and **IIa**

Molecules	Relative enthalpy [kJ/mol]		Relative free energy [kJ/mol]		Negative frequency [cm^{-1}]
	Gas	IEFPCM	Gas	IEFPCM	
Without solvent molecule					
inapH + pea	11.03	12.08	14.95	10.75	–
TS1	82.44	74.30	95.74	91.54	−88
IN1	64.85	42.27	86.03	69.77	–
TS2	117.62	115.52	143.48	137.70	−1469
IN2	12.86	4.463	29.63	29.64	–
TS3	54.87	45.16	67.67	71.34	−1318
Ia + water	0	0	0	0	–
Ia	0	0	0	0	–
TS4	116.31	109.74	117.77	108.59	−1462
IN3	105.28	94.78	105.18	95.74	–
TS5	137.31	139.67	142.95	138.49	−509
IN4	108.43	112.37	109.64	108.33	–
TS6	167.77	156.22	155.80	137.19	−1671
IIa + HCN	23.89	22.32	26.49	22.82	–
Added solvent molecule					
inapH + pea	8.93	11.03	12.86	13.12	–
TS1	61.44	59.60	65.90	76.66	−143
IN1	44.11	39.91	51.98	59.60	–
TS2	90.32	81.65	105.81	101.34	−1091
IN2	8.14	17.33	23.63	34.13	–
TS3	58.29	60.12	74.04	79.02	−652
Ia + water	0	0	0	0	–
Ia	0	0	0	0	–
TS4	75.35	67.47	89.27	84.01	−589
IN3	59.60	58.29	68.79	67.21	–
TS5	100.29	91.37	109.74	100.82	−1361
IN4	72.46	70.89	87.17	87.43	–
TS6	80.08	78.24	98.45	103.71	−725
IIa + HCN	28.09	28.88	29.67	23.10	–

and absolute energies of all molecules are listed in *Table S2*. In addition, the numbering of atoms is shown in *Fig. S5*. The first step in the mechanism without solvent molecule is formation of the appropriate carbinolamine (hemiaminal) intermediate *via* nucleophilic attack of the incoming amine nitrogen atom (N(2)) on the carbonyl carbon atom (C(2)) of the substrate. One of the H-atoms of the amine molecule forms a hydrogen bond with the C=O oxygen atom of inapH (H···O = 2.362 Å, *Table 3*). The attack of the pea molecule results in an interaction with the imine carbon atom through the oxygen atom. First, the nitrogen atom of pea approaches to the carbon atom of inapH, forming **IN1** through **TS1** transition state, and then at that position consequently it forms a four-membered ring transition structure (**TS2**). The energy barrier (E_a) of this step is quite high, being 137.70 kJ/mol. **TS2** transforms into the tetrahedral intermediate (a carbinolamine, **IN2**). The barrier for the formation of the carbinolamine intermediate is rather low at 29.64 kJ/mol, compared to **TS2**. In the species from inapH + pea to **IN2**, the distance between the C(2) and N(2) atoms changes from 4.060 to 1.493 Å, indicating formation of single bond between them. This is followed by the approach of the amine hydrogen to the OH oxygen to form **TS3** with a relatively high-energy barrier of 71.34 kJ/mol. In the subsequent stage (**Ia** + H_2O), the C–N bond distances shorten gradually from 1.493 to 1.291 Å, leading to the formation of the C=N imine double bond. The ΔH and ΔG values of the formation of the final oxiimine alcohol (**Ia**) are −11.03 and −14.95 kJ/mol in the gas phase, and −12.08 and −10.75 kJ/mol in the EtOH solution, respectively. On the other hand, in the mechanism of solvent added molecule, relative enthalpies and free energies of the all molecules are given in *Table 2*. Generally, in the presence of alcohol molecule in the mechanism, it was determined that the relative energies are lower than the mechanism without solvent molecule. Especially, the relative energies of transition state were reduced with the design of six-membered transition product. In fact, the formation of the title compound **Ia** is an equilibrium reaction with a calculated ΔG value of *ca.* −12 kJ/mol. These results suggest that compound **Ia** can only be obtained in a non-aqueous medium.

Table 3. The interatomic distances of the studied molecules for reaction of inapH and pea calculated using the B3LYP/6-311G(d,p) method

Formation of compound **Ia**

	İnapH + pea	TS1	IN1	TS2	IN2	TS3	**Ia** + H_2O
C1–N1	1.297	1.283	1.295	1.294	1.294	1.295	1.297
C1–C2	1.505	1.524	1.525	1.533	1.530	1.517	1.496
N1–O1	1.359	1.391	1.391	1.393	1.389	1.390	1.389
O1–Ha	1.087	1.014	1.013	1.013	1.016	1.015	1.016
C2–O2	1.213	1.231	1.484	1.368	1.441	1.672	3.438
C2–N2	4.060	2.032	1.518	1.518	1.493	1.390	1.291
N2–Hb	1.024	1.026	1.059	1.608	2.386	2.883	3.755
N2–Hc	1.014	1.028	1.041	1.032	1.028	1.543	2.372
C9–N2	1.489	1.496	1.521	1.490	1.479	1.466	1.471
O2–Ha	2.362	2.381	2.253	1.533	0.986	0.980	0.950
O2–Hb	3.715	2.701	3.223	2.799	2.542	1.237	0.962
O3–Hd							0.982
O1–Hd							6.001

Rearrangement of compound **Ia**, *formation of compound* **IIa**

	Ia + H_2O	TS4	IN3	TS5	IN4	TS6	**IIa** + HCN
C1–N1	1.297	1.290	1.155	1.154	1.153	1.162	1.153
C1–C2	1.496	1.502	1.460	1.505	1.491	1.643	3.750
N1–O1	1.389	1.397	3.013	3.365	4.421	3.394	4.134
O1–Ha	1.016	1.014	0.965	0.974	1.014	1.576	2.006
C2–N2	1.291	1.290	1.288	1.339	1.483	1.436	1.390
C9–N2	1.471	1.460	1.466	1.469	1.479	1.479	1.477
O3–Hd	0.982	1.797					
O3–He			1.011	0.973	0.983	0.978	0.980
O1–Hd	6.001	2.003	0.967	1.043	2.563	3.169	3.195
C2–O1		2.788	4.772	1.757	1.428	1.369	1.227
C1–Ha		3.022	3.248	3.146	2.622	1.448	1.067
N2–Hd		4.168	5.119	1.802	1.031	1.022	1.016

The natural bond orbital analysis (NBO) charges are given in *Table S3*. The positive NBO charge on the C(2) atom at **IN1** was smaller than that of the inapH + pea form because of its connection with the electronegative nitrogen atom (N(2)). The negative NBO charge on the N(2) atom at −0.875 in pea also gradually decreased from inapH + pea to **Ia** + H_2O, due to the nitrogen atom of pea binding to the C=O carbon atom. The NBO charge of C=O oxygen atom is −0.579 in inapH. This atom charge gradually increases from inapH + pea to **Ia** + H_2O, from −0.579 to −0.924. These results indicate that the H_2O molecule is away from the structure, thus the compound **Ia** is formed.

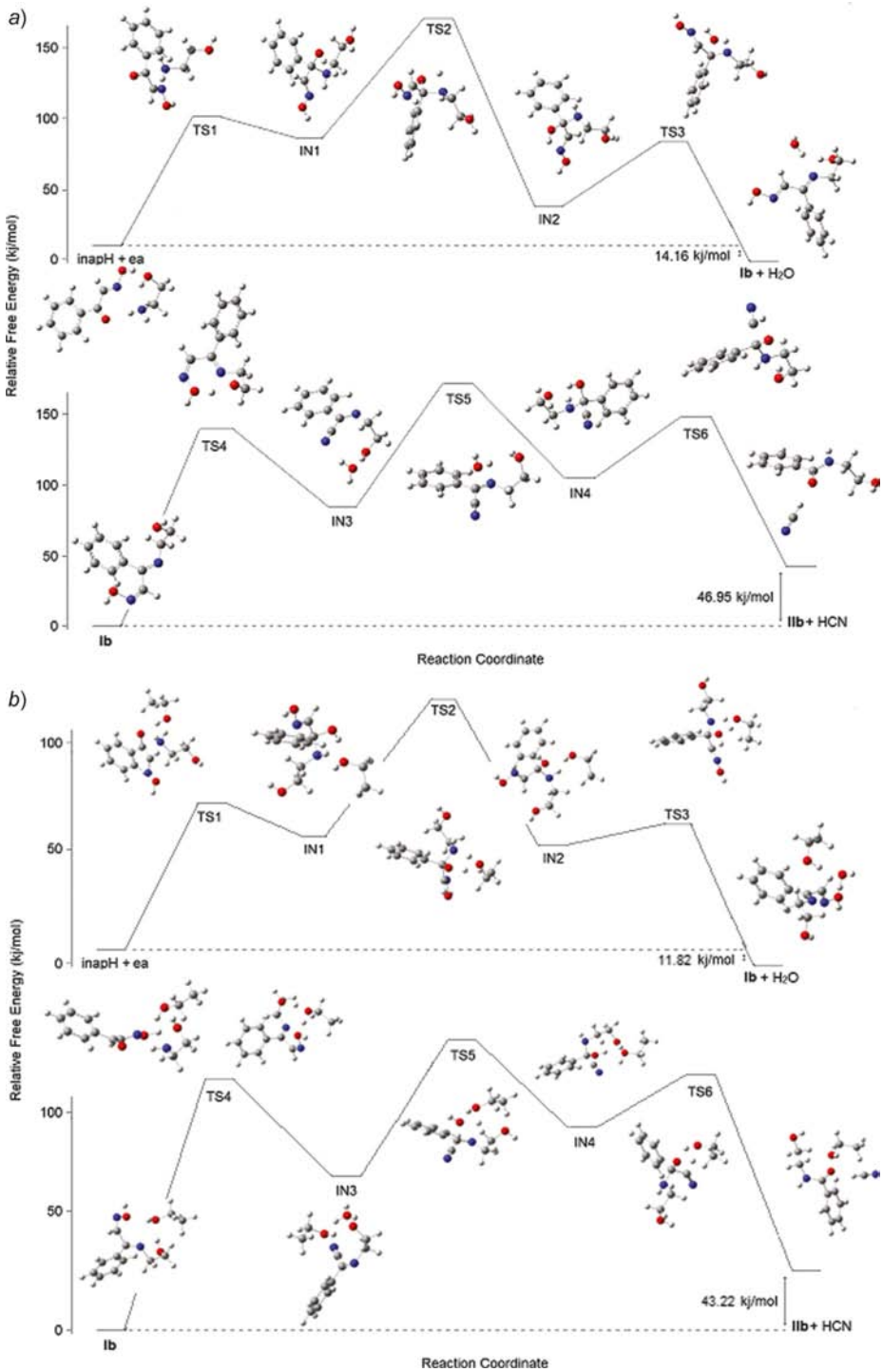

Fig. 3. The potential energy diagram and geometry transformations, showing the formation of compound **Ib**, **IIb**, and optimized geometries of the reactants, intermediates, transition states, and products calculated by B3LYP/6-311G(d,p), *a*) without solvent molecule, *b*) added solvent molecule.

Rearrangement of Compound **Ia** *and Formation of Compound* **IIa**

Theoretical calculations were carried out to study the rearrangement mechanism of oxiimine alcohol (**Ia**) in the presence of gas phase and EtOH solution. The mechanism of rearrangement was done three steps, namely: *i*) dehydration of oxime group (**Ia**-IN3 in *Fig. S6*), *ii*) water to attack the imine (TS5-IN4 in *Fig. S6*), and *iii*) removal of HCN to give the final amido alcohol (TS6-**IIa** + HCN in *Fig. S6*). As shown in *Fig. S6*, in the rearrangement mechanism of oxiimine alcohol (**Ia**), the hydroxyethyl hydrogen atom interacts with the oxime oxygen atom, and removes the H_2O molecule from oxime group in the first step (**Ia**, **TS4**, **IN3**). In this case, the N(1)–O(1) bond distance increases from 1.389 to 3.014 Å. Then, a H_2O molecule, as a nucleophile, attacks the imine C(2) atom, and forms the tetrahedral intermediate **IN4** through transition-state **TS5**. The C(1)–O(1) distance was found to be 1.428 Å in **IN4**, while calculated 4.772 Å in **IN3**. This bond distance is 1.757 Å in **TS5**. The negative charge on the O(1) atom decreased, while the positive charge on C(2) atom also increased at **TS5**. Using the B3LYP/6-311G(d,p) method, the activation barrier of this step was quite high, being 138.49 kJ/mol. This energy barrier was calculated at 100.82 kJ/mol in the six-membered transition state. The negative imaginary frequency was found only at −509 and −1361 cm^{-1} for **TS5** (*Table 2*). In the last step, the transfer of hydrogen atom of OH group at that position consequently forms a four-membered ring transition structure (**TS6**). The energy barrier (E_a) of this step is quite high, being 137.19 kJ/mol. During the formation of the **IIa** + HCN, the C(1)–C(2) bond distance changes from 1.496 to 3.750 Å. Formally, the dissociation of the C(1)–C(2) bond occurs in the last step, giving a free amido alcohol (**IIa**) and HCN. In addition, as a result of rearrangements the N(2)–Hd bond distance decrease from 4.168 to 1.016 Å. The ΔG value calculated for the rearrangement mechanism of oxiimine alcohol (**Ia**) is *ca*. 28 and 23 kJ/mol in gas phase and EtOH solution, respectively. These results indicate that the presence of excess H_2O molecules favors the formation of the compound **IIa** as expected. As described previously [69], this result was confirmed experimentally during the synthesis of an oxiimine alcohol (**IIa**).

Table 4. Relative enthalpy, relative free energy, and negative frequency of the structures of the reaction paths for gas phase and EtOH solution of compound **Ib** and **IIb**

Molecules	Relative enthalpy [kJ/mol]		Relative free energy [kJ/mol]		Negative frequency [cm^{-1}]
	Gas	IEFPCM	Gas	IEFPCM	
Without solvent molecule					
inapH + ea	15.75	8.93	13.38	14.16	–
TS1	132.06	95.83	130.88	101.51	−80
IN1	95.04	68.79	100.45	83.67	–
TS2	157.53	147.81	174.16	163.93	−1554
IN2	39.12	18.64	54.03	32.52	–
TS3	89.00	48.31	89.70	65.31	−1839
Ib + water	0	0	0	0	–
Ib	0	0	0	0	–
TS4	148.60	144.14	147.67	140.59	−1423
IN3	73.25	70.10	66.62	64.52	–
TS5	157.79	158.32	164.20	157.90	−1115
IN4	95.83	96.09	101.25	96.26	–
TS6	150.44	143.88	150.03	136.39	−1426
IIb + HCN	46.47	50.41	45.11	46.95	–
Added solvent molecule					
inapH + ea	7.09	6.04	13.39	11.82	–
TS1	86.12	58.55	85.85	68.26	−140
IN1	68.79	49.62	77.45	59.60	–
TS2	104.23	91.89	119.98	111.58	−1355
IN2	34.13	32.56	49.09	47.52	–
TS3	41.74	33.87	55.39	53.56	−753
Ib + water	0	0	0	0	–
Ib	0	0	0	0	–
TS4	105.54	101.34	107.64	105.81	−352
IN3	83.23	60.12	69.57	62.49	–
TS5	122.61	128.65	122.08	129.17	−1319
IN4	94.52	94.52	90.05	89.00	–
TS6	127.33	103.18	117.36	107.64	−1525
IIb + HCN	62.22	43.06	47.52	43.32	–

The positive NBO charge on the C(2) atom gradually increases from 0.280 to 0.704 during the rearrangement. The negative NBO charge on the O(1) atom at −0.519 in **IIa** first increases until **IN3**, and then decreases at 0.684, due to the removal of H_2O molecule. The positive NBO charge of C(1) atom first increases until **IN3**, and then gradually decreases at 0.084, due to removal of HCN group from compound **Ia**. These results indicate that the HCN molecule is away from the structure, thus the compound **IIa** may be formed in this solution environment in which equal amount of H_2O occurs to oxiimine alcohol molecule (**Ia**). While this amount of H_2O is not enough for the hydrolysis of oxiimine alcohol molecule (**Ia**), it is sufficient for the formation of amido alcohol molecule (**IIa**).

Formation of Compound **Ib**

Theoretical calculations were also carried out to study the formation mechanism of compound **Ib** in gas phase and EtOH solution. The mechanism of the formation reaction of compound **Ib** is given in *Fig. S4*. The corresponding potential energy surfaces (PES's) and optimized structures of all molecules for the formation reaction of the compounds **Ib** and **IIb** are shown in *Fig. 3*, while relative enthalpies and free relative energies of the reactants, intermediates (IN), transition states (TS), and products are given in *Table 4* and absolute energies of all molecules are listed in *Table S4*. As shown in *Fig. S4*, in the formation of compound **Ib**, the first step is the ea molecule, as a nucleophile, attacks the C=O carbon atom. This results in an unstable product with a negatively charged O(2) atom (−0.896) and N(2) atom (−0.582), which simultaneously transfers the H-atom to the O(2) atom. As a result, a carbinolamine intermediate (**IN2**) is formed. During the formation of the **IN2**, the C–N bond distance changes from 4.191 to 1.450 Å. Formally, the other H-atom is transferred to the O(2) atom and then the dissociation of the C–O bond occurs in the next steps, giving oxiimine alcohol (**Ib**) and H_2O molecule. The ΔG value calculated for the formation of the compound **Ib** is *ca.* −13 and −14 kJ/mol in gas phase and EtOH solution, respectively, being quite similar to that calculated for the formation of **Ia**. Other selected bond lengths and the NBO charges calculated at B3LYP/6-311G(d,p) level are given in *Tables 5* and *S4*.

Table 5. The interatomic distances of the studied molecules for reaction of inapH and ea calculated using the B3LYP/6-311G(d,p) method

Formation of compound **Ib**

	İnapH + ea	TS1	IN1	TS2	IN2	TS3	**Ib** + H_2O
C1–N1	1.280	1.270	1.272	1.268	1.267	1.268	1.278
C1–C2	1.491	1.512	1.507	1.532	1.525	1.505	1.475
N1–O1	1.353	1.402	1.406	1.402	1.397	1.400	1.386
O1–Ha	0.993	0.963	0.962	0.963	0.963	0.963	0.963
C2–O2	1.222	1.236	1.484	1.380	1.426	1.796	3.649
C2–N2	4.191	2.029	1.519	1.518	1.450	1.376	1.284
N2–Hb	1.016	1.015	1.026	1.606	3.035	2.921	3.252
N2–Hc	1.011	1.017	1.027	1.020	1.012	1.343	1.973
C9–N2	1.471	1.479	1.495	1.477	1.468	1.466	1.457
O2–Hb	2.406	2.484	2.214	1.535	0.969	0.969	0.962
O2–Hc	3.918	2.622	3.222	2.501	2.660	1.315	0.975
O3–Hd							0.963
O1–Hd							5.813

Rearrangement of compound **Ib**, *Formation of compound* **IIb**

	Ib + H_2O	TS4	IN3	TS5	IN4	TS6	**IIb** + HCN
C1–N1	1.278	1.299	1.154	1.154	1.153	1.171	1.150
C1–C2	1.475	1.476	1.462	1.459	1.495	1.581	4.182
N1–O1	1.386	1.391	2.929	3.479	2.351	3.277	4.176
O1–Ha	0.963	0.960	0.962	0.969	0.977	1.575	1.947
C2–N2	1.284	1.285	1.275	1.292	1.453	1.403	1.360
C9–N2	1.457	1.456	1.442	1.460	1.462	1.455	1.458
O3–Hd	0.963	1.725					
O3–He			0.965	0.962	0.965	0.963	0.962
O1–Hd	5.813	2.021	0.970	1.256	2.653	3.207	3.145
C2–O1		2.732	4.494	2.011	1.416	1.410	1.230
C1–Ha		3.141	2.805	3.060	2.499	1.447	1.080
N2–Hd		3.421	4.366	1.708	1.014	1.013	1.007

Rearrangement of Compound **Ib***, Formation of Compound* **IIb**

The mechanism of the formation of the compound **IIb** involves three steps as in the mechanism of the formation of the compound **IIa**, namely: *i*) dehydration of oxime group (**Ib**-IN3 in *Fig S6*), *ii*) H_2O to attack the imine (**TS5**-IN4 in *Fig S6*), and *iii*) removal of HCN to give the final amido alcohol (**TS6**-**IIb** + HCN in *Fig S6*). For these three steps, there are three transition states, namely **TS4**, **TS5**, and **TS6**. The activation barriers of these transition states were quite high, being 140.59, 157.90, and 136.39 kJ/mol, respectively, and negative imaginary frequencies were found to be 1423, 1115, and 1426 cm^{-1} for each transition states, respectively. These energy barriers of transition states were calculated at 105.81, 129.17, and 107.64 kJ/mol in mechanism of added solvent molecule. During the formation of the **IIb** + HCN, the C(1)–C(2) bond distance changes from 1.475 to 4.182 Å. Formally, the dissociation of the C(1)–C(2) bond occurs in the last step, giving a free amido alcohol (**IIb**) and HCN. In addition, as a result of rearrangements, the N(2)–Hd bond distance decreases from 3.421 to 1.007 Å. The ΔG values calculated for the rearrangement mechanism of oxiimine alcohol (**Ib**) are 45.11 and 46.95 kJ/mol in gas phase and EtOH solution, respectively. These driving forces are relatively high compared with the rearrangement mechanism of oxiimine alcohol (**Ia**). Also, the driving force is higher than *ca.* 45 kJ/mol in EtOH solution. This result indicates that the compound **IIb** cannot be experimentally synthesized from the rearrangement of oxiimine alcohol (**Ib**) as in [70].

The Effect of Dispersion Correction

DFT is among the most popular and versatile methods available in computational chemistry. It provides an appropriate and feasible level of theory for several problems supporting experimental research. However, a limitation in DFT is the ability to describe dispersion and the energies of all molecules in a sufficient way. Development has been done to treat this nontrivial matter. Excellent reviews on dispersion interactions in DFT are given by

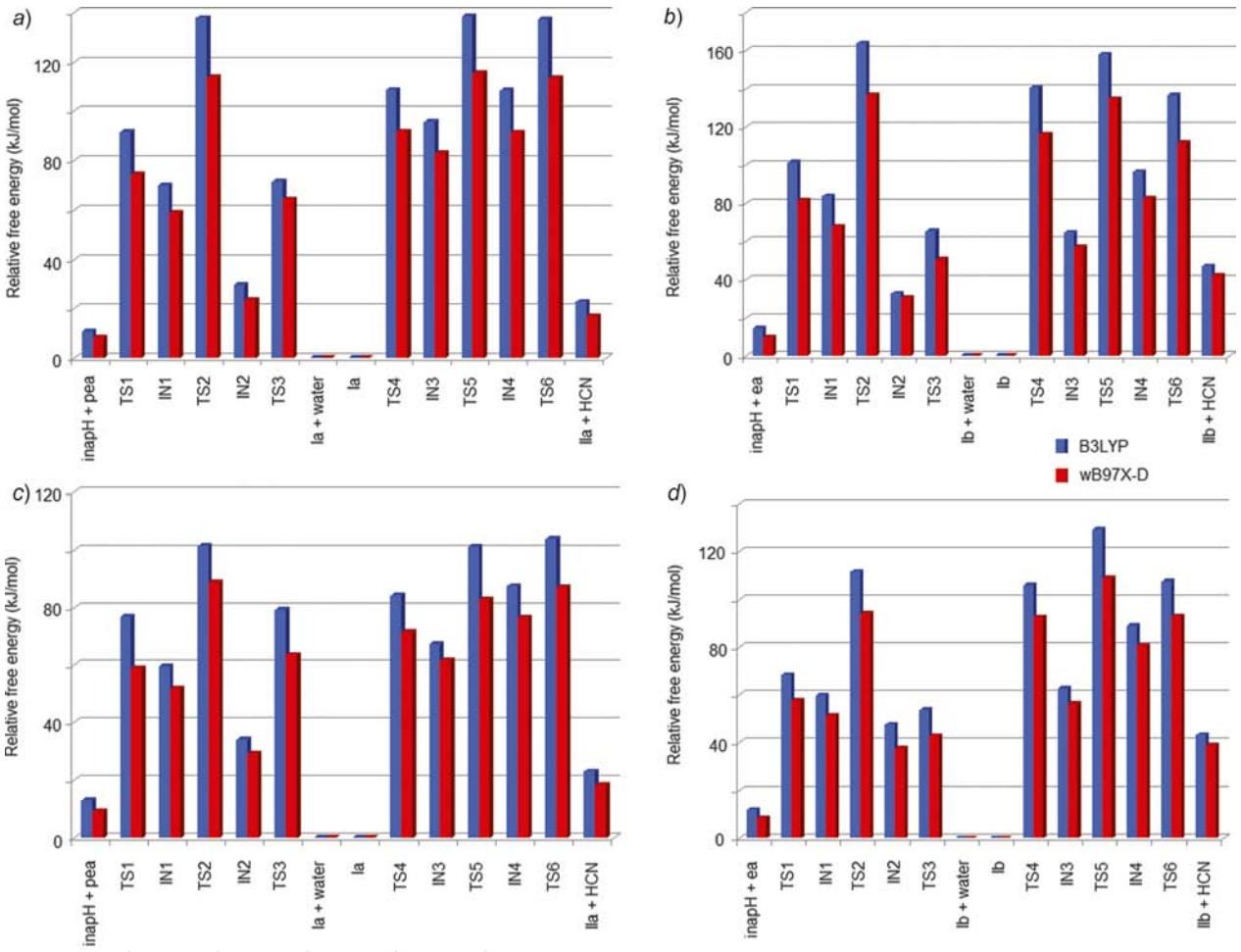

Fig. 4. Comparison of *Gibbs* free energy for the mechanisms with different functionals without dispersion correction (B3LYP) and added dispersion correction (wB97X-D): *a*) formation **IIa**, *b*) **IIb** without solvent molecule, and *c*) formation **IIa**, *d*) **IIb**-added solvent molecule.

Johnson et al. [71] and *Grimme* [72], including the widely accepted scheme by *Grimme* of dispersion-corrected DFT which are DFT-D [73][74] and DFT-D3 [75]. Therefore, all the calculations were also performed by wB97X-D method and 6-311G(d,p) basis set. Calculation of the relative free energies of all the molecules in the mechanisms is listed in *Table S5*, while comparison of the *Gibbs* free energy values calculated by the method of B3LYP and wB97X-D is presented in *Fig. 4*. The first and second columns in *Table S5* show the relative free energies calculated with B3LYP and wB97X-D, respectively, for **Ia** and **IIa**, while the third and fourth columns present the relative free energies performed with B3LYP and wB97X-D, respectively, for **Ib** and **IIb**. In general, the relative free energies of all molecules calculated from wB97XD method lower than performed from B3LYP level. The largest difference of relative *Gibbs* free energy between B3LYP and wB97X-D methods is 24.92 kJ/mol which is observed in TS6 energy barrier of the reaction of **Ib** to **IIb** without solvent molecule, while the smallest difference is 2.34 kJ/mol in the **IN2** of same reaction. In addition, the ΔG values calculated by wB97X-D/6-311G(d,p) for the formation of the compound **Ia** and **Ib** are *ca.* −9 kJ/mol for both ways. On the other hand, the *Gibbs* free energies of formation of **IIa** from **Ia** were determined 16.88 and 18.38 kJ/mol for without and added solvent molecule, respectively, while the ΔG values of reaction **Ib** to **IIb** were calculated 41.83 and 38.86 kJ/mol, respectively. These results are quite similar to that of calculated by B3LYP.

Table 6. *Gibbs* free energy changes of the structures of the formation reaction of **I** and **II** at the different temperatures

	ΔG				
	100	200	298.15	400	500
inapH + *pea* → **Ia** → **IIa**					
inapH + pea	9.98	12.34	14.95	17.59	18.90
TS1	76.93	86.38	95.74	109.48	123.13
IN1	72.46	80.08	86.03	93.73	101.34
TS2	124.18	133.90	143.48	159.10	171.97
IN2	20.22	24.94	29.63	35.97	42.27
TS3	51.46	59.60	67.67	81.39	95.04
Ia + water	0	0	0	0	0
Ia	0	0	0	0	0
TS4	108.43	113.16	117.77	112.37	110.01
IN3	107.91	106.59	105.18	102.39	99.50
TS5	135.21	139.15	142.95	148.34	153.59
IN4	106.59	108.17	109.64	110.01	110.27
TS6	147.55	151.75	155.8	153.85	153.33
IIa + HCN	25.20	26.25	26.49	24.42	15.75
inapH + *ea* → **Ib** → **IIb**					
inapH + ea	9.71	10.76	13.38	14.44	16.80
TS1	127.07	128.38	130.88	131.01	131.54
IN1	93.20	96.62	100.45	102.39	107.38
TS2	163.57	169.34	174.16	179.58	189.30
IN2	50.41	53.30	54.03	55.66	59.86
TS3	87.17	89.53	89.7	90.58	93.99
Ib + water	0	0	0	0	0
Ib	0	0	0	0	0
TS4	140.46	146.24	147.67	145.98	142.56
IN3	58.55	64.59	66.62	64.06	61.17
TS5	150.18	158.84	164.2	165.14	167.50
IN4	88.74	97.40	101.25	101.34	102.92
TS6	139.94	147.03	150.03	149.39	148.86
IIb + HCN	43.32	44.37	45.11	41.22	33.61

Thermodynamic Properties

The statistical thermodynamics can be obtained theoretically from theoretical frequencies of studied reactions and molecules. The *Gibbs* free energies (G) of all molecules were calculated by the theoretical harmonic frequencies of the optimized molecules at B3LYP/6-311G(d,p) level. The changes of *Gibbs* free energy (ΔG) at various temperatures, which are 100 – 500 K, were listed in *Table 6*. While the formations of **Ia** and **Ib** are an exothermic process, the **IIa** and **IIb** are positive, so these reaction are endothermic. The ΔG values are predicted to be 25.20 and 43.32 kJ/mol at 100 K for formations of **IIa** and **IIb**, respectively. These relative free energies are fallen down to 15.75 and 33.61 kJ/mol, respectively. In the course of formations of **IIa** and **IIb**, the calculated ΔG decreases with increasing temperature. These results show that the final rearrangement products, namely **IIa** and **IIb**, can be obtained easier at higher temperatures.

Natural Bond Orbital Analysis for All Compounds

Natural bond orbital analysis have been calculated at B3LYP/6-311G(d,p) level using *Gaussian 03*. *Table 7* presents the resulted natural atomic hybrids centered on atom A (h_A) on some atoms with the polarization coefficient c_A for each hybrid (in parentheses) in the corresponding NBO [76]. The results are summarized as follows:

I) Similar results were obtained in the orbital analysis of both molecules, therefore, it is sufficient to discuss only one molecule.

II) The sp^2 characters of C and N $\sigma_{C(1)–N(1)}$ bond orbitals in inapH + pea decrease with increasing reaction coordinate from inapH + pea to **IN3**, so the characters of carbon and nitrogen bond orbitals are $sp^{1.14}$ and $sp^{1.04}$, respectively, which results in formation of C≡N bond.

III) The character of the C(2) atom in $\sigma_{C(1)–C(2)}$ bond of inapH + pea is $sp^{1.99}$. The p character of this hybrid orbital was firstly increased ($sp^{2.66}$) in **IN1**, and then decreased again value of $sp^{1.87}$ in **Ia** molecule. These results supports first the disappearance of the carbonyl bond (C(2)=O(2)), and then the formation of the imine bond (C(2)=N(2)).

IV) In the rearrangement mechanism of oxiimine alcohol (**Ia**), the hydroxyethyl hydrogen atom interacts with the oxime O(1) atom, resulting in the removal of the H_2O molecule from oxime group in the first step (**Ia**,

Table 7. NBO calculated hybridizations for all molecules calculated at B3LYP/6-311G(d,p)

Molecules	C1–N1	C1–C2	N1–O1	C2–O2	C9–N2	C2–N2	C2–O1
a							
inapH + pea	$sp^{2.02}$, $sp^{1.36}$	$sp^{1.93}$, $sp^{1.99}$	$sp^{4.43}$, $sp^{3.56}$	$sp^{2.26}$, $sp^{1.34}$	$sp^{3.09}$, $sp^{2.09}$	–	–
TS1	$sp^{2.01}$, $sp^{1.46}$	$sp^{1.89}$, $sp^{2.11}$	$sp^{5.14}$, $sp^{3.61}$	$sp^{2.22}$, $sp^{1.30}$	$sp^{3.17}$, $sp^{2.47}$	–	–
IN1	$sp^{2.01}$, $sp^{1.31}$	$sp^{1.86}$, $sp^{2.66}$	$sp^{5.15}$, $sp^{3.86}$	$sp^{3.40}$, $sp^{3.63}$	$sp^{3.63}$, $sp^{2.49}$	$sp^{4.24}$, $sp^{2.25}$	–
TS2	$sp^{1.97}$, $sp^{1.37}$	$sp^{1.91}$, $sp^{2.71}$	$sp^{5.09}$, $sp^{3.63}$	$sp^{3.41}$, $sp^{2.65}$	$sp^{3.18}$, $sp^{2.29}$	$sp^{3.79}$, $sp^{2.73}$	–
IN2	$sp^{2.02}$, $sp^{1.28}$	$sp^{1.95}$, $sp^{2.85}$	$sp^{5.01}$, $sp^{3.76}$	$sp^{3.72}$, $sp^{2.14}$	$sp^{3.03}$, $sp^{2.22}$	$sp^{3.06}$, $sp^{1.98}$	–
TS3	$sp^{2.02}$, $sp^{1.44}$	$sp^{1.89}$, $sp^{2.62}$	$sp^{4.96}$, $sp^{3.62}$	–	$sp^{2.94}$, $sp^{2.14}$	$sp^{2.31}$, $sp^{1.86}$	–
Ia	$sp^{2.02}$, $sp^{1.37}$	$sp^{2.25}$, $sp^{1.87}$	$sp^{5.11}$, $sp^{3.64}$	–	$sp^{3.13}$, $sp^{2.25}$	$sp^{2.03}$, $sp^{1.38}$	–
TS4	$sp^{1.96}$, $sp^{1.41}$	$sp^{2.42}$, $sp^{1.70}$	$sp^{5.34}$, $sp^{3.70}$	–	$sp^{3.08}$, $sp^{2.27}$	$sp^{1.93}$, $sp^{1.43}$	–
IN3	$sp^{1.14}$, $sp^{1.04}$	$sp^{0.87}$, $sp^{2.36}$	–	–	$sp^{3.01}$, $sp^{2.15}$	$sp^{1.88}$, $sp^{1.48}$	–
TS5	$sp^{1.11}$, $sp^{1.08}$	$sp^{0.90}$, $sp^{2.28}$	–	–	$sp^{3.12}$, $sp^{2.35}$	$sp^{1.91}$, $sp^{1.59}$	–
IN4	$sp^{1.11}$, $sp^{1.07}$	$sp^{0.89}$, $sp^{3.16}$	–	–	$sp^{2.96}$, $sp^{2.00}$	$sp^{2.93}$, $sp^{1.94}$	$sp^{3.66}$, $sp^{2.28}$
TS6	$sp^{1.33}$, $sp^{1.04}$	$sp^{0.81}$, $sp^{5.06}$	–	–	$sp^{3.32}$, $sp^{2.11}$	$sp^{2.87}$, $sp^{1.89}$	$sp^{3.03}$, $sp^{2.38}$
IIa	–	–	–	–	$sp^{3.26}$, $sp^{1.86}$	$sp^{2.17}$, $sp^{1.84}$	$sp^{2.23}$, $sp^{1.49}$
b							
inapH + pea	$sp^{2.02}$, $sp^{1.36}$	$sp^{1.92}$, $sp^{1.98}$	$sp^{4.34}$, $sp^{3.51}$	$sp^{2.27}$, $sp^{1.34}$	$sp^{3.07}$, $sp^{2.13}$	–	–
TS1	$sp^{1.95}$, $sp^{1.32}$	$sp^{1.81}$, $sp^{2.06}$	$sp^{5.34}$, $sp^{3.82}$	$sp^{2.28}$, $sp^{1.30}$	$sp^{3.16}$, $sp^{2.28}$	–	–
IN1	$sp^{2.03}$, $sp^{1.32}$	$sp^{1.88}$, $sp^{2.70}$	$sp^{5.11}$, $sp^{3.85}$	$sp^{3.45}$, $sp^{3.72}$	$sp^{3.56}$, $sp^{2.43}$	$sp^{4.28}$, $sp^{2.28}$	–
TS2	$sp^{1.94}$, $sp^{1.29}$	$sp^{1.84}$, $sp^{2.71}$	$sp^{5.30}$, $sp^{3.83}$	$sp^{3.40}$, $sp^{2.44}$	$sp^{3.20}$, $sp^{2.10}$	$sp^{3.87}$, $sp^{2.53}$	–
IN2	$sp^{2.01}$, $sp^{1.28}$	$sp^{1.95}$, $sp^{2.85}$	$sp^{5.00}$, $sp^{3.75}$	$sp^{3.72}$, $sp^{2.14}$	$sp^{3.01}$, $sp^{2.26}$	$sp^{3.05}$, $sp^{1.97}$	–
TS3	$sp^{1.91}$, $sp^{1.33}$	$sp^{1.82}$, $sp^{2.27}$	$sp^{5.29}$, $sp^{3.81}$	–	$sp^{3.05}$, $sp^{2.30}$	$sp^{2.29}$, $sp^{1.72}$	–
Ib	$sp^{2.02}$, $sp^{1.37}$	$sp^{1.88}$, $sp^{2.24}$	$sp^{5.13}$, $sp^{3.64}$	–	$sp^{3.09}$, $sp^{2.28}$	$sp^{2.02}$, $sp^{1.38}$	–
TS4	$sp^{2.07}$, $sp^{1.56}$	$sp^{1.33}$, $sp^{1.90}$	$sp^{5.34}$, $sp^{3.69}$	–	$sp^{3.07}$, $sp^{2.26}$	$sp^{1.81}$, $sp^{1.50}$	–
IN3	$sp^{1.14}$, $sp^{1.04}$	$sp^{0.87}$, $sp^{2.35}$	–	–	$sp^{3.02}$, $sp^{2.18}$	$sp^{1.88}$, $sp^{1.48}$	–
TS5	$sp^{1.12}$, $sp^{1.08}$	$sp^{0.89}$, $sp^{2.26}$	–	–	$sp^{3.08}$, $sp^{2.39}$	$sp^{1.95}$, $sp^{1.44}$	–
IN4	$sp^{1.11}$, $sp^{1.06}$	$sp^{0.89}$, $sp^{3.15}$	–	–	$sp^{2.95}$, $sp^{2.06}$	$sp^{2.97}$, $sp^{1.97}$	$sp^{3.61}$, $sp^{2.27}$
TS6	$sp^{1.30}$, $sp^{1.13}$	$sp^{0.81}$, $sp^{3.97}$	–	–	$sp^{3.10}$, $sp^{2.17}$	$sp^{2.69}$, $sp^{1.76}$	$sp^{3.53}$, $sp^{2.48}$
IIb	–	–	–	–	$sp^{3.22}$, $sp^{1.88}$	$sp^{2.18}$, $sp^{1.65}$	$sp^{2.26}$, $sp^{1.50}$

TS4, **IN3**). The character of C(2) atom in $\sigma_{C(2)–N(2)}$ bond of **Ia** is $sp^{2.03}$. Then, a H_2O molecule attacks the imine C(2) atom as a nucleophile, and forms the C(2)–O(1) bond in tetrahedral intermediate **IN4**. In the **IN4**, the p character of the C(2) atom has increased by $sp^{3.66}$ (in $\sigma_{C(2)–O(1)}$). With the formation C=O bond, the character of the C(2) atom has returned again to sp^2 hybridization ($sp^{2.23}$).

Conclusions

In this work, the formation mechanisms of compounds **Ia** and **Ib**, and its rearrangement mechanisms in gas phase and EtOH solution were studied using the DFT at the B3LYP/6-311G(d,p) level of calculations with the solvent effects using the IEFPCM continuum model. The rate-determining steps are the nucleophilic attack of the pea and ea molecules to the C=O carbon atom of inapH, and then formation of the carbinolamine intermediates (**IN2**). The formation of compound **Ia** results in inapH and pea with ΔG values of −14.95 and −10.75 kJ/mol, and ΔG values of compound **Ib** were calculated at −13.38 and −14.16 kJ/mol in the gas and EtOH solution, respectively. These results suggest that the compound **Ia** and **Ib** obtained in a non-aqueous medium. The driving forces of rearrangement of compound **Ia** (formation of compound **IIa**) are calculated to be 26.49 and 22.82 kJ/mol in the gas and EtOH solution, respectively. These results indicate that the presence of excess water molecules favors the formation of the compound **IIa** as expected. As described earlier, this was observed experimentally during the synthesis of compound **IIa**. On the other hand, formation of compound **IIb** results in rearrangement of compound **Ib** with ΔG values of 45.11 and 46.95 kJ/mol. This high-energy barrier supports that the compound **IIb** cannot obtained from rearrangement of compound **Ib**. In addition, the mechanism studies were also performed on the participation of solvent molecules. Generally, in the presence of alcohol molecule in the mechanism, it was determined that the relative energies are lower than the mechanism without solvent molecule. On the other hand, dispersion corrections for reaction heat and free-energy barrier for the all molecules were estimated using the wB97X-D/6-311G(d,p) method. The relative free energies of all molecules calculated from wB97XD method lower than performed from B3LYP level. The statistical thermodynamic parameters were obtained from the theoretical harmonic frequencies at different temperatures, which are 100 – 500 K, and the results show that the final rearrangement products, namely **IIa** and **IIb**, can be obtained easier at high temperatures. The NBO calculated hybridization of selected bonds for all molecules shows that all of molecules have sp^x hybridization. The total hybridization of all molecules is sp^x that was confirmed by structure.

Computational Details

In the present work, the *Becke–Lee–Yang–Parr* functional (B3LYP) method [77] was adopted and all calculations were performed using the *Gaussian* 03 program package [78]. In the first step of the calculation, conformational features of **I** and **II** were studied to described the lowest energy conformers of **I** and **II**. All conformational properties were calculated at the 6-311G(d,p) basis set. Then, calculations of neutral formation mechanism of **I** and **II** were performed using the 6-311G(d,p) basis set. Harmonic frequencies of the structures were calculated at the same method and basis set to find local minima (all positive force constants) or transition states (one imaginary force constant only). The intrinsic reaction coordinate (IRC) calculation has been used to determine the true transition structure. The optimized gas-phase geometries have been used for B3LYP/6-311G(d,p) single point SCRF calculations. The IEFPCM and EtOH solvent have been used for SCRF calculations [79 – 81]. As the DFT functionals poorly describe dispersion effects, dispersion correction for reaction heat and free-energy barrier were estimated using the wB97X-D/6-311G(d,p) method developed by *Grimme* and co-workers [75]. NBO analysis and the thermodynamic properties for the all molecules throughout mechanism with temperature ranging from 100 to 500 K were performed in the gas phase at B3LYP method with the standard 6-311G(d,p) basis set.

Supplementary Data

Optimized geometries of isomers, atomic contributions of HOMO and LUMO orbitals, NBO charges, and total and relative energies of the molecules can be found in the supporting information. This is available free of charge *via* the internet at http://onlinelibrary.wiley.com.

This work is a part of a research project KUAP(F)-2015/20. We thank *Uludag University* for the financial support given to the project.

REFERENCES

[1] A. Chakravorty, *Coord. Chem. Rev.* **1974**, *13*, 1.
[2] M. E. Keeney, K. Osseo-Asare, K. A. Woode, *Coord. Chem. Rev.* **1984**, *59*, 141.
[3] V. Y. Kukushkin, D. Tudela, A. J. L. Pombeiro, *Coord. Chem. Rev.* **1996**, *156*, 333.
[4] V. Y. Kukushkin, A. J. L. Pombeiro, *Coord. Chem. Rev.* **1999**, *181*, 147.
[5] A. G. Smith, P. A. Tasker, D. J. White, *Coord. Chem. Rev.* **2003**, *241*, 61.
[6] P. Chaudhuri, *Coord. Chem. Rev.* **2003**, *243*, 143.
[7] C. J. Milios, T. C. Stamatatos, S. P. Perlepes, *Polyhedron* **2006**, *25*, 134.
[8] H. Nakamura, Y. Iitaka, H. Sakakibara, H. Umezawa, *J. Antibiot.* **1974**, *27*, 894.
[9] H. A. Kirst, E. F. Szymanski, D. E. Doman, J. L. Occolowitz, N. D. Jones, M. O. Chaney, R. L. Hamill, M. M. Hoehn, *J. Antibiot.* **1975**, *28*, 286.
[10] V. V. Ponomareva, N. K. Halley, X. Kou, N. N. Gerasimchuk, K. V. Domasevich, *J. Chem. Soc. Dalton Trans.* **1996**, 2351.
[11] T. W. Hambley, E. C. H. Ling, S. O'Mara, M. J. McKeage, P. J. Russell, *J. Biol. Inorg. Chem.* **2000**, *5*, 675.
[12] A. G. Quiroga, L. Cubo, E. de Blas, P. Aller, C. Navarro-Ranninger, *J. Inorg. Biochem.* **2007**, *101*, 104.
[13] S. Zorbas-Seifried, M. A. Jakupec, N. V. Kukushkin, M. Groessl, C. G. Hartinger, O. Semenova, H. Zorbas, V. Y. Kukushkin, B. K. Kepler, *Mol. Pharmacol.* **2007**, *71*, 357.
[14] Y. Y. Scaffidi-Domianello, K. Meelich, M. A. Jakupec, V. B. Arion, V. Y. Kukushkin, M. Galanski, B. K. Kepler, *Inorg. Chem.* **2010**, *49*, 5669.
[15] R. Glaser, A. Streitwieser, *J. Am. Chem. Soc.* **1988**, *111*, 7340.
[16] P. G. Kolandaivel, N. Kuze, T. Sakaizumi, O. Ohashi, K. Iijima, *J. Phys. Chem. A* **1997**, *101*, 2873.
[17] P. Kolandaivel, K. Senthilkumar, *J. Mol. Struct. (Theochem)* **2001**, *535*, 61.
[18] P. I. Nagy, J. Kökösi, A. Gergely, Á. Rácz, *J. Phys. Chem. A* **2003**, *107*, 7861.
[19] I. Georgieva, N. Trendafilova, *Chem. Phys.* **2006**, *321*, 311.
[20] S. Nsikabaka, W. Harb, M. F. Ruiz-López, *J. Mol. Struct. (Theochem)* **2006**, *764*, 161.
[21] A. R. Bekhradnia, S. Arshadi, *Monatsh. Chem.* **2007**, *138*, 725.
[22] H. Tavakol, S. Arshadi, *J. Mol. Model.* **2009**, *15*, 807.
[23] A. V. Afonin, I. A. Ushakov, D. V. Pavlov, A. V. Ivanov, A. I. Mikhaleva, *Magn. Reson. Chem.* **2010**, *48*, 685.
[24] J. Grzegorzek, Z. Mielke, *Eur. J. Org. Chem.* **2010**, 5301.
[25] L. D. Popov, S. I. Levchenkov, I. N. Shcherbakov, V. A. Kogan, Y. P. Tupolova, *Russ. J. Gen. Chem.* **2010**, *80*, 493.
[26] J. Jayabharathi, A. Manimekalai, M. Padmavathy, *Med. Chem. Res.* **2011**, *20*, 981.
[27] F. Azarakhshi, D. Nori-Shargh, N. Masnabadi, H. Yahyaei, S. N. Mousavi, *Phosp. Sulf. Silic. Relat. Elem.* **2012**, *187*, 276.
[28] U. Sayin, Ö. Dereli, E. Türkkan, A. Ozmen, *Radiat. Phys. Chem.* **2012**, *81*, 146.
[29] G. P. Li, W. R. Xu, X. J. Lin, C. B. Liu, *Chin. Chem. Lett.* **2006**, *17*, 423.
[30] J. Wang, J. Gu, J. Leszczynski, M. Feliks, W. A. Sokalski, *J. Phys. Chem. B* **2007**, *111*, 2404.
[31] K. Sharma, S. B. Mishra, A. K. Mishra, *Helv. Chim. Acta* **2011**, *94*, 2256.
[32] A. P. Guimarães, T. C. C. França, T. C. Ramalho, M. N. Rennó, E. F. Ferreira da Cunha, K. S. Matos, D. T. Mancini, K. Kuča, *J. Appl. Biomed.* **2011**, *9*, 163.
[33] T. Stepanenko, L. Lapinski, M. J. Nowak, L. Adamowicz, *Vibrat. Spectr.* **2001**, *26*, 65.
[34] K. Sohlberg, K. D. Dobbs, *J. Mol. Struct. (Theochem)* **2002**, *577*, 137.
[35] K. Malek, M. Vala, H. Kozłowski, L. M. Proniewicz, *Magn. Reson. Chem.* **2004**, *42*, 23.
[36] B. Golec, Z. Mielke, *J. Mol. Struct.* **2007**, *844–845*, 242.
[37] B. Golec, J. Grzegorzek, Z. Mielke, *Chem. Phys.* **2008**, *353*, 13.
[38] T. Irshaidat, *Tetrahedron Lett.* **2008**, *49*, 631.
[39] N. V. Istomina, N. A. Shcherbina, L. B. Krivdin, *Russ. J. Org. Chem.* **2009**, *45*, 481.
[40] V. Arjunan, C. V. Mythili, K. Mageswari, S. Mohan, *Spectrochim. Acta A* **2011**, *79*, 245.
[41] N. R. Gonewar, V. B. Jadhav, K. D. Jadhav, R. G. Sarawadekar, *Res. Pharm.* **2012**, *2*, 18.
[42] N. E. Hall, B. J. Smith, *J. Phys. Chem. A* **1998**, *102*, 4930.
[43] B. Szefczyk, P. Kedzierski, W. A. Sokalski, J. Leszczynski, *Mol. Phys.* **2006**, *104*, 2203.
[44] S. H. Üngören, M. Saçmacı, C. Arıcı, E. Şahin, T. Arslan, F. Kandemirli, *Phosp.Sulf. Silic. Relat. Elem.* **2009**, *184*, 2877.
[45] Z. Önal, I. Yildirim, F. Kandemirli, T. Arslan, *Struct. Chem.* **2010**, *21*, 809.

[46] J. Ortega-Catro, M. Adrover, J. Frau, A. Savlà, J. Donoso, F. Muñoz, *J. Phys. Chem. A* **2010**, *114*, 4634.
[47] E. Erdtman, E. A. C. Bushnell, J. W. Gauld, L. A. Eriksson, *Comput. Theor. Chem.* **2011**, *963*, 479.
[48] C. Solís-Calero, J. Ortega-Castro, A. Hernández-Laguna, F. Muñoz, *Theor. Chem. Acc.* **2012**, *131*, 1263.
[49] T. H. Lowry, K. S. Richardson, 'Mechanism and Theory in Organic Chemistry', Harper & Row Publishers Inc., 1976.
[50] R. Opsahl, 'Kirk Othmer Encyclopaedia of Chemical Technology', 4th Edn., Vol. 2, J. Wiley, 1999.
[51] A. Aguilo, C. Hobbs, E. G. Zey, 'Ulmann's Encyclopaedia of Industrial Chemistry', 6th Edn., J. Wiley, 1998.
[52] R. A. Nugent, C. H. Hall, 'Kirk Othmer Encyclopedia of Chemical Technology', 4th Edn., Vol. 2, J. Wiley, 1999.
[53] S. C. Mitchel, R. H. Waring, 'Ulmann's Encyclopaedia of Industrial Chemistry', 6th Edn., J. Wiley, 1998.
[54] T. Horlenko, J. R. Fritch, O. S. Fruchey, Hoechst Celanese Corporation, US Pat. 4954652, 1990.
[55] Y. Ogata, M. Okano, K. Matsumoto, *J. Am. Chem. Soc.* **1955**, *77*, 4643.
[56] F. Greer, D. E. Pearson, *J. Am. Chem. Soc.* **1955**, *77*, 6649.
[57] P. J. McNulty, D. E. Pearson, *J. Am. Chem. Soc.* **1959**, *81*, 612.
[58] M. I. Vinnik, N. G. Zarakhani, *Russ. Chem. Rev.* **1967**, *36*, 51.
[59] B. J. Gregory, R. B. Moodie, K. Schofield, *J. Chem. Soc. B* **1970**, 338.
[60] S.-G. Kim, T. Kawakami, T. Ando, Y. Yukawa, *Bull. Chem. Soc. Jpn.* **1979**, *52*, 1115.
[61] G. Petrini, G. Leonfanti, M. A. Mantegazza, F. Pignataro, in 'Green Chemistry', Eds. P. T. Anastas and T. C. Williamson, American Chemical Society, 1996.
[62] S. Tonti, P. Roffia, V. Gervasutti, to Enichem Anic S.p.A., EP, 0496385A1, 1992.
[63] J. Roeseler, W. Hoelderich, D. Arntz, to Degussa AG. DE, 19608 660.4, 1996.
[64] W. F. Holderich, G. Dahloff, H. Ichihashi, K. Sugita, to Sumitomo Chemical Company US Pat., 6,531,595 B2, 2003.
[65] G. Dahlhoff, J. P. M. Niederer, W. F. Hoelderich, *Catal. Rev. Sci. Eng.* **2001**, *43*, 381.
[66] T. Okubo, S. Suzuki, T. Matsushita, T. Suzuki, to Sumitomo Chemical Co. EP 2157080, 2009.
[67] X. Liu, L. Xiao, H. Wua, Z. Li, J. Chen, C. Xia, *Catal. Commun.* **2009**, *10*, 424.
[68] A. Zicmanis, S. Katkevica, P. Mekss, *Catal. Commun.* **2009**, *10*, 614.
[69] Y. Kaya, G. Irez, H. Mutlu, O. Buyukgungor, *Synth. React. Inorg. Met. Org. Chem.* **2011**, *41*, 754.
[70] Y. Kaya, C. Icsel, V. T. Yilmaz, O. Buyukgungur, *J. Organomet. Chem.* **2014**, *752*, 83.
[71] E. R. Johnson, I. D. Mackie, G. A. DiLabio, *J. Phys. Org. Chem.* **2009**, *22*, 1127.
[72] S. Grimme, *WIREs Comput. Mol. Sci.* **2011**, *1*, 211.
[73] S. Grimme, *J. Comput. Chem.* **2004**, *25*, 1463.
[74] S. Grimme, *J. Comput. Chem.* **2006**, *27*, 1787.
[75] S. Grimme, J. Antony, S. Ehrlich, H. Krieg, *J. Phys. Chem.* **2010**, *132*, 154104.
[76] A. E. Reed, L. A. Curtiss, F. Weinhold, *Chem. Rev.* **1988**, *88*, 899.
[77] A. D. Becke, *J. Chem. Phys.* **1993**, *98*, 5648.
[78] M. J. Frisch, G. W. Trucks, H. B. Schlegel, G. E. Scuseria, M. A. Robb, J. R. Cheeseman, J. A. Montgomery Jr, T. Vreven, K. N. Kudin, J. C. Burant, J. M. Millam, S. S. Iyengar, J. Tomasi, V. Barone, B. Mennucci, M. Cossi, G. Scalmani, N. Rega, G. A. Petersson, H. Nakatsuji, M. Hada, M. Ehara, K. Toyota, R. Fukuda, J. Hasegawa, M. Ishida, T. Nakajima, Y. Honda, O. Kitao, H. Nakai, M. Klene, X. Li, J. E. Knox, H. P. Hratchian, J. B. Cross, V. Bakken, C. Adamo, J. Jaramillo, R. Gomperts, R. E. Stratmann, O. Yazyev, A. J. Austin, R. Cammi, C. Pomelli, J. W. Ochterski, P. Y. Ayala, K. Morokuma, G. A. Voth, P. Salvador, J. J. Dannenberg, V. G. Zakrzewski, S. Dapprich, A. D. Daniels, M. C. Strain, O. Farkas, D. K. Malick, A. D. Rabuck, K. Raghavachari, J. B. Foresman, J. V. Ortiz, Q. Cui, A. G. Baboul, S. Clifford, J. Cioslowski, B. B. Stefanov, G. Liu, A. Liashenko, P. Piskorz, I. Komaromi, R. L. Martin, D. J. Fox, T. Keith, M. A. Al-Laham, C. Y. Peng, A. Nanayakkara, M. Challacombe, P. M. W. Gill, B. Johnson, W. Chen, M. W. Wong, C. Gonzalez, J. A. Pople, Gaussian 03, Revision E.01, Gaussian, Inc., Wallingford, CT, 2004.
[79] E. Cancès, B. Mennucci, J. Tomasi, *J. Chem. Phys.* **1997**, *107*, 3032.
[80] B. Mennucci, E. Cancès, J. Tomasi, *J. Phys. Chem. B* **1997**, *101*, 10506.
[81] B. Mennucci, J. Tomasi, *J. Chem. Phys.* **1997**, *106*, 5151.

Received June 22, 2015
Accepted February 4, 2016

